The Astrophysical Journal, 585:885–889, 2003 March 10

HIGH-ENERGY EMISSION FROM THE PROMPT GAMMA-RAY BURST

Dafne Guetta[1] and Jonathan Granot[2]
Received 2002 August 7; accepted 2002 November 20

ABSTRACT

We study the synchrotron and synchrotron self-Compton (SSC) emission from internal shocks that are responsible for the prompt gamma-ray emission in gamma-ray bursts (GRBs) and consider the relation between these two components, taking into account the high-energy cutoff due to pair production and Thomson scattering. We find that in order for the peak energy of the synchrotron to be $E_p \sim 300$ keV with a variability time $t_v \gtrsim 1$ ms, a Lorentz factor of $\Gamma \lesssim 200$ is needed, implying no high-energy emission above $\sim$30 MeV and the synchrotron component dominating at all energies. If we want both $E_p \sim 300$ keV and prompt high-energy emission up to $\sim$2 GeV, as detected by EGRET for GRB 940217, we need $\Gamma \sim 600$ and $t_v \sim 0.1$ ms, which might be resolved by Super Agile. If such prompt high-energy emission is common in GRBs, as may be tested by the *Gamma-Ray Large Area Space Telescope* (*GLAST*), then for $t_v \gtrsim 1$ ms, we need $\Gamma \gtrsim 350$, which implies $E_p \lesssim 100$ keV. Therefore, if X-ray flashes are GRBs with high values of t_v and Γ, they should produce $\gtrsim 1$ GeV emission. For an electron power-law index $p > 2$, the SSC component dominates the emission above $\sim$100 MeV. Future observations by *GLAST* may help determine the value of p and whether the high-energy emission is consistent with a single power law (implying that one component, the synchrotron, is dominant) or has a break where the νF_ν slope turns from negative to positive, which implies that the SSC component becomes dominant above $\sim$100 MeV. The high-energy emission is expected to show similar variability and time structure to that of the soft gamma-ray emission. Finally, we find that in order to see delayed high-energy emission from the prompt GRB due to pair production with the cosmic IR background, extremely small intergalactic magnetic fields ($\lesssim 10^{-22}$ G) are required.

Subject headings: gamma rays: bursts — ISM: jets and outflows — radiation mechanisms: nonthermal

1. INTRODUCTION

The leading models of gamma-ray bursts (GRBs) involve a relativistic flow emanating from a compact central source, where the prompt gamma-ray emission is attributed to internal shocks within the outflow itself that arise from variability in its Lorentz factor, while the afterglow results from an external shock that is driven into the ambient medium as it decelerates the original ejecta (Rees & Mészáros 1994; Sari & Piran 1997). In this so called "internal-external" shock model, the duration of the prompt GRB is directly related to the time during which the central source is active. The most popular emission mechanism is synchrotron radiation from relativistic electrons accelerated in the shocks, which radiate in the strong magnetic fields (close to equipartition values) within the shocked plasma. An additional radiation mechanism that may also play an important role is synchrotron self-Compton (SSC) emission, which is the upscattering of the synchrotron photons by the relativistic electrons to much higher energies.

The synchrotron and SSC components from internal shocks have been considered in previous works in various contexts. Papathanassiou & Mészáros (1996) studied the emission from internal shocks, focusing on the comparison between internal and external shocks. Pilla & Loeb (1998) calculated the spectrum from internal shocks taking into account multiple Compton scattering and pair production. They show the broadband spectrum for a fixed radius of collision R and varying Lorentz factor Γ of the outflow, and for a fixed Γ and a varying R. Our treatment differs in that we assume different free parameters, namely, the Lorentz factor Γ and the variability time t_v of the central engine that emits the outflow, rather than Γ and R. Under our assumptions, the radius of collision scales as $R \sim 2\Gamma^2 c t_v \propto \Gamma^2$ and is not independent of Γ. This results in different conclusions as to the relation between the prompt gamma-ray emission in the BATSE range and the emission at higher energies, which is the main subject of our work. Panaitescu & Mészáros (2000) explored the possibility that the prompt gamma-ray emission in the BATSE range arises from the SSC component rather than the synchrotron, where the latter is in the optical or UV range. Recently, Dai & Lu (2002) studied the SSC emission from internal shocks, concentrating on the possible interaction of high-energy photons with the IR background (see § 3).

In this paper we calculate the high-energy emission during the prompt GRB from internal shocks for both the synchrotron and SSC components and consider the relations between these two components. We estimate the high-energy cutoff and study the constraints on the model parameters that arise from the requirement that E_p (the typical photon energy of the synchrotron component) be in the BATSE range.

The synchrotron and SSC spectra are calculated in § 2, and expressions are provided for the break frequencies and flux normalization. In § 3 we derive the constraints on the model that arise from the optical depth to pair production

[1] Osservatorio Astrofisico di Arcetri, Largo E. Fermi 2, I-50125 Florence, Italy; dafne@arcetri.astro.it.
[2] Institute for Advanced Study, Olden Lane, Princeton, NJ 08540; granot@ias.edu.

and to Thomson scattering. We consider the recent claim for a possible delayed emission due to the pair production of high-energy photons with the IR background (Dai & Lu 2002), and we show that in order for this radiation to be detectable, a very small ($\lesssim 10^{-22}$ G) intergalactic magnetic field (IGMF) is needed. Our results are discussed in § 4.

2. THE SYNCHROTRON AND SSC EMISSION

The Lorentz factor of the flow, Γ, is assumed to vary on a timescale t_v and with a typical amplitude of $\Delta\Gamma \sim \Gamma$. The collisions between the shells typically occur at a radius

$$R \approx 2\Gamma^2 c t_v = 6\times 10^{13}\Gamma_{2.5}^2 t_{v,-2}\ \mathrm{cm}\ , \tag{1}$$

where $\Gamma_{2.5} = \Gamma/10^{2.5}$ and $t_{v,-2} = t_v/(10^{-2}\ \mathrm{s})$. The internal energy that is released in each collision between shells is distributed among electrons, magnetic fields, and protons with fractions ϵ_e, ϵ_B, and $1-\epsilon_e-\epsilon_B$, respectively. Since the electrons are typically in the fast-cooling regime (as is shown below), the luminosity $L = (\Omega_j/4\pi)L_{\rm iso}$ (where Ω_j is the solid angle of the GRB outflow) of a single pulse, which corresponds to a single collision between two shells within the outflow, is equal to the rate at which energy is given to the electrons by the internal shock.[3] The internal shocks are expected to be at least mildly relativistic, so that we can assume that in the rest frame of the shocked fluid, the velocity of the shock is close to that for a relativistic shock, $c/3$. The local frame luminosity is $L' = L/\Gamma^2 = \Omega_j R^2 \epsilon_e e' c/3$, and the internal energy density is given by

$$e' \approx \frac{3L_{\rm iso}}{4\pi R^2 c\Gamma^2 \epsilon_e} = 2.2\times 10^8 \epsilon_e^{-1} L_{52}\Gamma_{2.5}^{-6} t_{v,-2}^{-2}\ \mathrm{ergs\ cm^{-3}}\ , \tag{2}$$

where $L_{\rm iso} = L_{52}10^{52}$ ergs s^{-1}. Primed quantities are measured in the local rest frame of the shocked fluid, while unprimed quantities are measured in the observer frame.

For a mildly relativistic shock, the internal energy behind the shock is similar to the rest energy:

$$n' \approx \frac{e'}{m_p c^2} \approx 1.5\times 10^{11}\epsilon_e^{-1} L_{52}\Gamma_{2.5}^{-6} t_{v,-2}^{-2}\ \mathrm{cm^{-3}}\ . \tag{3}$$

The magnetic field is

$$B' = \sqrt{8\pi\epsilon_B e'} \approx 7.5\times 10^4 \epsilon_e^{-1/2}\epsilon_B^{1/2} L_{52}^{1/2}\Gamma_{2.5}^{-3} t_{v,-2}^{-1}\ \mathrm{G}\ . \tag{4}$$

The electrons are accelerated in the shock to a power-law distribution of energies: $N(\gamma) = dn'/d\gamma \propto \gamma^{-p}$ for γ in the range $\gamma_m < \gamma < \gamma_M$. The minimum Lorentz factor is given by

$$\gamma_m = \left(\frac{p-2}{p-1}\right)\frac{\epsilon_e e'}{n' m_e c^2} \approx \left(\frac{p-2}{p-1}\right)\frac{m_p}{m_e}\epsilon_e \approx 610 f_p \epsilon_e\ , \tag{5}$$

where $f_p \equiv 3(p-2)/(p-1)$.

[3] The fact that we refer to the flux of a single pulse, rather than the time-average flux of all the pulses throughout the burst, results in a factor of 3 difference in the expression for the internal energy. However, since this kind of calculation is accurate anyway only up to factors of the order of unity, similar uncertainties result from the unknown details of the outflow, and factors of (at least) the order of unity are expected between different collisions between shells in the same GRB, the exact choice of the parameterization of the luminosity is not very important.

The electrons radiatively cool by the combination of the synchrotron and SSC processes, the timescales of which are $t'_{\rm syn} \sim 6\pi m_e c/\sigma_{\rm T} B'^2 \gamma_e$ and $t_{\rm SC} = t_{\rm syn}/Y$, the combined cooling time being $t'_c = (1/t'_{\rm syn} + 1/t'_{\rm SC})^{-1} = t'_{\rm syn}/(1+Y)$, where

$$Y \approx \begin{cases} \epsilon_e/\epsilon_B\ , & \epsilon_e \ll \epsilon_B\ , \\ \sqrt{\epsilon_e/\epsilon_B}\ , & \epsilon_e \gg \epsilon_B\ , \end{cases} \tag{6}$$

is the Compton y-parameter (Sari, Piran, & Narayan 1996). The maximum Lorentz factor of the electrons γ_M and the cooling Lorentz factor γ_c are set by equating t'_c with the acceleration time, $\sim 2\pi\gamma_e m_e c/qB'$ (where q is the electric charge of the electron), and the dynamical time, $t'_{\rm dyn} = R/c\Gamma \approx 2\Gamma t_v$, respectively:

$$\gamma_M = \sqrt{\frac{3q}{B'\sigma_{\rm T}(1+Y)}} \approx 1.7\times 10^5 \frac{\epsilon_e^{1/4}\Gamma_{2.5}^{3/2} t_{v,-2}^{1/2}}{\sqrt{1+Y}\,\epsilon_B^{1/4} L_{52}^{1/4}}\ , \tag{7}$$

$$\gamma_c = \frac{6\pi\Gamma m_e c^2}{(1+Y)B'^2\sigma_{\rm T} R} \approx 0.02\frac{\epsilon_e \Gamma_{2.5}^5 t_{v,-2}}{(1+Y)\epsilon_B L_{52}}\ . \tag{8}$$

Obviously, $\gamma_c < 1$ no longer corresponds to the Lorentz factor of the electrons and instead represents the fraction of the dynamical time (the shell shock crossing time for internal shocks) during which the electrons cool to a nonrelativistic random Lorentz factor. In this case, the electrons are relativistic only within a thin layer behind the shock of width $\gamma_c\Delta'$, where Δ' is the width of the shell, and are cold (i.e., nonrelativistic) in the rest of the shell. As can be seen from equations (5) and (8), typically $\gamma_c \ll \gamma_m$, and the electrons are fast cooling.

The synchrotron frequency and the total synchrotron power of a single electron are given by

$$\nu_{\rm syn} = \nu_0\gamma_e^2 = \Gamma\frac{3q_e B'\gamma_e^2}{16 m_e c}\ , \quad P_{e,\rm syn} = \Gamma^2\frac{4}{3}\sigma_{\rm T} c\frac{B'^2}{8\pi}\gamma_e^2\ , \tag{9}$$

where $\nu'_{\rm syn} = \nu_{\rm syn}/\Gamma$ and $P'_{e,\rm syn} = P_{e,\rm syn}/\Gamma^2$. The self-absorption frequency is typically $\max(\nu_c,\ \nu_0) < \nu_{\rm sa} < \nu_m$, and the absorption coefficient is given by

$$\alpha'_{\nu'} \approx \frac{3\gamma_c n'\left(P'_{e,\rm syn}/\nu'_{\rm syn}\right)}{16\pi m_e(\nu')^{5/3}(\nu'_0)^{1/3}}\left(\frac{16 m_e c\nu'}{3qB'}\right)^{-4/3}\ . \tag{10}$$

We solve $\alpha'_{\nu'_{\rm sa}}\Delta' = 1$ for $\nu'_{\rm sa}$, where $\Delta' \approx R/\Gamma$ is the width of the shell in the local frame, and then we have $\nu_{\rm sa} = \Gamma\nu'_{\rm sa}$. The synchrotron frequencies are given by

$$\begin{aligned}
\nu_c &= 3.7\times 10^{10}(1+Y)^{-2}\epsilon_e^{3/2}\epsilon_B^{-3/2} L_{52}^{-3/2}\Gamma_{2.5}^8 t_{v,-2}\ \mathrm{Hz}\ ,\\
\nu_0 &= 7.8\times 10^{13}\epsilon_e^{-1/2}\epsilon_B^{1/2} L_{52}^{1/2}\Gamma_{2.5}^{-2} t_{v,-2}^{-1}\ \mathrm{Hz}\ ,\\
\nu_{\rm ac} &= 5.7\times 10^{13} f_p^{-8/5}(1+Y)^{-3/5}\epsilon_e^{-9/5}\\
&\quad\times \epsilon_B^{-2/5} L_{52}^{1/5}\Gamma_{2.5}^{-1/5} t_{v,-2}^{-2/5}\ \mathrm{Hz}\ ,\\
\nu_{\rm sa} &= 2.0\times 10^{16}(1+Y)^{-1/3}\epsilon_e^{-1/3} L_{52}^{1/3}\Gamma_{2.5}^{-1} t_{v,-2}^{-2/3}\ \mathrm{Hz}\ ,\\
\nu_m &= 2.9\times 10^{19} f_p^2 (1+Y)^{-1/3}\epsilon_e^{3/2}\epsilon_B^{1/2} L_{52}^{1/2}\Gamma_{2.5}^{-2} t_{v,-2}^{-1}\ \mathrm{Hz}\ ,\\
\nu_M &= 2.3\times 10^{24}(1+Y)^{-1}\Gamma_{2.5}\ \mathrm{Hz}\ ,
\end{aligned} \tag{11}$$

and the synchrotron spectrum is[4]

$$\frac{\nu F_\nu}{\nu_m F_{\nu_m}} = \begin{cases} \left(\frac{\nu_{sa}}{\nu_m}\right)^{1/2}\left(\frac{\nu_{ac}}{\nu_{sa}}\right)^{19/8}\left(\frac{\nu}{\nu_{ac}}\right)^3 , & \nu < \nu_{ac} , \\ \left(\frac{\nu_{sa}}{\nu_m}\right)^{1/2}\left(\frac{\nu}{\nu_{sa}}\right)^{19/8} , & \nu_{ac} < \nu < \nu_{sa} , \\ \left(\frac{\nu}{\nu_m}\right)^{1/2} , & \nu_{sa} < \nu < \nu_m , \\ \left(\frac{\nu}{\nu_m}\right)^{(2-p)/2} , & \nu_m < \nu < \nu_M , \end{cases} \tag{12}$$

where from the normalization condition, we obtain

$$\frac{L_{iso}}{4\pi D^2} = \int_0^\infty d\nu\, F_\nu = 6 f_p^{-1} \nu_m F_{\nu_m} , \tag{13}$$

$$\nu_m F_{\nu_m} = \frac{f_p L_{iso}}{24\pi D^2} = 1.3 \times 10^{-6} f_p L_{52} D_{28}^{-2} \text{ ergs cm}^{-2}\text{ s}^{-1} , \tag{14}$$

where $D = 10^{28} D_{28}$ cm is the distance to the GRB.

The SSC spectrum is given by

$$\frac{\nu F_\nu^{SC}}{Y \nu_m F_{\nu_m}} = \begin{cases} \left(\frac{\nu_{sa}^{SC}}{\nu_m^{SC}}\right)^{1/2}\left(\frac{\nu}{\nu_{sa}^{SC}}\right)^2 , & \nu < \nu_{sa}^{SC} , \\ \left(\frac{\nu}{\nu_m^{SC}}\right)^{1/2} , & \nu_{sa}^{SC} < \nu < \nu_m^{SC} , \\ \left(\frac{\nu}{\nu_m^{SC}}\right)^{1-p/2} , & \nu_m^{SC} < \nu < \nu_{KN}^{SC} , \\ \left(\frac{\nu_{KN}^{SC}}{\nu_m^{SC}}\right)^{1-p/2}\left(\frac{\nu}{\nu_{KN}^{SC}}\right)^{1/2-p} , & \nu_{KN}^{SC} < \nu < \nu_M^{SC} , \end{cases} \tag{15}$$

where $\nu_{sa}^{SC} \equiv \max(\gamma_c^2,\ 1)\nu_{sa}$ and

$$\begin{aligned} \nu_m^{SC} &= \gamma_m^2 \nu_m = 1.1 \times 10^{25} f_p^4 \epsilon_e^{7/2} \epsilon_B^{1/2} L_{52}^{1/2} \Gamma_{2.5}^{-2} t_{v,-2}^{-1} \text{ Hz} , \\ \nu_{KN}^{SC} &= \frac{\Gamma^2 m_e^2 c^4}{h^2 \nu_m} \\ &= 5.2 \times 10^{25} f_p^{-2} \epsilon_e^{-3/2} \epsilon_B^{-1/2} L_{52}^{-1/2} \Gamma_{2.5}^4 t_{v,-2} \text{ Hz} , \\ \nu_M^{SC} &= \frac{\Gamma \gamma_M m_e c^2}{h} \\ &= 6.6 \times 10^{27} (1+Y)^{-1/2} \epsilon_e^{1/4} \epsilon_B^{-1/4} L_{52}^{-1/4} \Gamma_{2.5}^{5/2} t_{v,-2}^{1/2} \text{ Hz} . \end{aligned} \tag{16}$$

If $\nu_{KN}^{SC} < \nu_m^{SC}$, then we have $\nu F_\nu \propto \nu^{1/2-p}$ for $\nu_{KN}^{SC} < \nu < \nu_M^{SC}$. For details about the spectrum above the Klein-Nishina frequency, ν_{KN}^{SC}, see Guetta & Granot (2003).

[4] If there is significant mixing of the shocked fluid (which may be the case if there is strong turbulence), then we will have $F_\nu \propto \nu^2$ immediately below ν_{sa}, instead of $F_\nu \propto \nu^{11/8}$ for $\nu_{ac} < \nu < \nu_{sa}$ and $F_\nu \propto \nu^2$ below $\nu_{ac} = \nu_{sa}(\nu_c/\nu_m)^{4/5}$ (Granot, Piran, & Sari 2000). However, this will not have any significant effect on the SSC spectrum, and since ν_{sa} is typically below the observational window, it will be quite difficult to distinguish between these two possibilities observationally.

3. THE HIGH-ENERGY CUTOFF

In order for high-energy photons to escape the system and reach the observer, they must overcome a few potential obstacles along the way. Inside the source, there are two main constraints: (1) the opacity of the high-energy photons to pair production due to interaction with lower energy photons, $\tau_{\gamma\gamma}$, must be smaller than 1 in order for high-energy photons to escape, and (2) the Thomson optical depth due to pair production, τ_p, must be smaller than unity in order for the observed prompt GRB emission to escape and reach the observer. These effects have been studied by several different authors (Sari & Piran 1997; Lithwick & Sari 2001; Guetta, Spada, & Waxman 2001). Outside of the source, high-energy photons ($\gtrsim$500 GeV) may interact with photons from the cosmic IR background to produce pairs (Salamon & Stecker 1998; Dai & Lu 2002).

We reparameterize the expressions of Lithwick & Sari (2001) for $\tau_{\gamma\gamma}$ and τ_p, using our parameters, and express the requirements $\tau_{\gamma\gamma} < 1$ and $\tau_p < 1$ as constraints on the Lorentz factor Γ:

$$\Gamma > 69(\epsilon_e^3 \epsilon_B)^{(p-2)/8(p+1)} (L_{52}^{p+2} t_{v,-2}^{-2p} \epsilon_{max}^{2p})^{1/8(p+1)} \quad (\tau_{\gamma\gamma} < 1) , \tag{17}$$

$$\Gamma > 170(\epsilon_e^3 \epsilon_B)^{(p-2)/2(3p+4)} (L_{52}^{1/2} t_{v,-2})^{(p+2)/(3p+4)} \quad (\tau_p < 1) , \tag{18}$$

where ε_{max} is the maximal energy of a photon that can escape (measured in the observer frame in units of $m_e c^2$) and the numerical coefficients are for $p = 2.5$ but do not vary by more than 10% for $2.05 < p < 2.9$. In order to see the soft gamma rays from the prompt GRB, the inequality in equation (18) must be satisfied, in which case there is an upper cutoff at $\nu_{\gamma\gamma} = \epsilon_{max} m_e c^2/h$, corresponding to a photon energy

$$h\nu_{\gamma\gamma} = 2.6(\epsilon_e^3 \epsilon_B)^{(2-p)/2p} L_{52}^{-(p+2)/2p} \Gamma_{2.5}^{4(p+1)/p} t_{v,-2} \text{ GeV} , \tag{19}$$

where the numerical coefficient is for $p = 2.5$ and varies by less than 10% for $2.17 < p < 2.67$. The maximum photon energy detected by EGRET during the prompt emission is ~3 GeV (Hurley et al. 1994), for which equation (17) implies $\Gamma > 370$ for our fiducial parameters.

In Figure 1 we show the synchrotron and SSC νF_ν spectra for different values of Γ and t_v. As can be seen from this figure, the high-energy cutoff is typically determined by the opacity to pair production and is given by equation (19). As mentioned above, the high-energy photons ($\gtrsim$500 GeV) that escape the source may still interact with the cosmic IR background and produce pairs. However, as illustrated in Figure 1, in order for photons in this energy range to leave the system, one needs $\Gamma \gtrsim 600$ and $t_v \gtrsim 0.01$ s, which, in turn, implies $h\nu_m = E_p \lesssim 1$ keV. Therefore, this effect is expected to be irrelevant for typical GRBs, with E_p in the BATSE range, and might play a role only for the low end of the E_p distribution of the X-ray flashes.

It has recently been claimed (Dai & Lu 2002) that a delayed emission on a timescale of $\Delta t \sim 10^3$ s after the GRB may result because of the inverse Compton upscattering of the cosmic microwave background (CMB) by the pairs produced by the interaction of photons with energies $\gtrsim$300 GeV emitted during the prompt GRB and the cosmic IR background. The pairs are produced at a typical distance of $R_{pair} \approx 5.8 \times 10^{24}$ cm and lose their

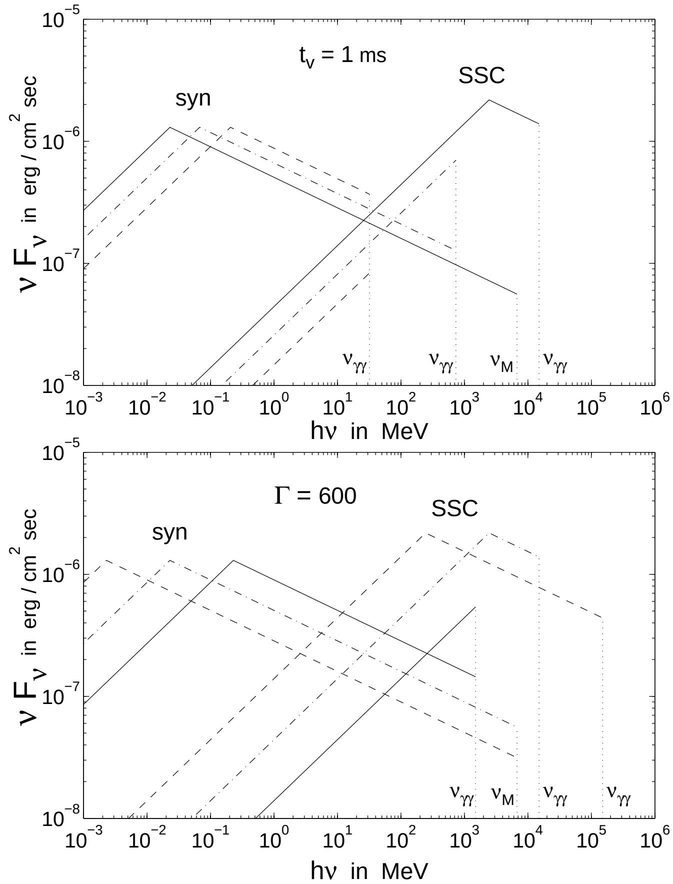

FIG. 1.—Plot of the νF_ν spectrum from the prompt GRB for the synchrotron and SSC components, including the relevant high-energy cutoff among the possibilities discussed in the text. In the top panel we fix $t_v = 1$ ms, and the dashed, dot-dashed, and solid lines correspond to $\Gamma = 200$, 350, and 600, respectively. In the bottom panel we fix $\Gamma = 600$, and the dashed, dot-dashed, and solid lines correspond to $t_v = 10$, 1, and 0.1 ms, respectively. In both panels we use $L_{52} = 1$ and $p = 2.5$, as well as $\epsilon_e = 0.45$ and $\epsilon_B = 0.1$, where the latter were chosen so that the peak of νF_ν of the synchrotron would be in the right range (Guetta et al. 2001).

energy by upscattering CMB photons over a length scale of $R_{\rm IC} \approx 7.3 \times 10^{24}$ cm. Dai & Lu estimated the delay time by $\Delta t \sim R/2\gamma_e^2$, where $R = \max(R_{\rm pair},\ R_{\rm IC})$. This estimate is based on the fact that the pairs that are produced initially propagate almost in the same direction as a high-energy photon (i.e., in a radial direction from the GRB) and on the assumption that they do not change their direction by more than $1/\gamma_e$ over $R_{\rm IC}$. However, the presence of IGMFs $B_{\rm IG}$ at $R_{\rm pair}$ causes a deflection angle of

$$\theta_{\rm def} = \frac{R_{\rm IC}}{R_{\rm L}} = 1.4 \times 10^5 \left(\frac{B_{\rm IG}}{10^{-11}\ {\rm G}}\right)\left(\frac{\gamma_e}{3 \times 10^5}\right)^{-2}, \quad (20)$$

where $R_{\rm L} = \gamma_e m_e c^2/qB$ is the Larmor radius of the electron. In order for the above estimate for Δt not to be effected by this deflection, we need $\theta_{\rm def} < 1/\gamma_e$, which according to equation (20) implies $B_{\rm IG} < B_0 = 2.3 \times 10^{-22}$ G. For $B_{\rm IG} > B_0$, the value of Δt increases by a factor of $\sim(B_{\rm IG}/B_0)^2$ compared to the estimate of Dai & Lu. For $\theta_{\rm def} > 1$, i.e., $B_{\rm IG} \gtrsim 10^{-16}$ G, we expect $\Delta t \sim R_{\rm IC}/c \sim 10^7$ yr and a roughly isotropic emission. Therefore, the detection of such a delayed emission will suggest an IGMF $\lesssim 10^{-21}$ G at a distance of a few Mpc from the site of the GRB, while the lack of detection of this emission will imply a larger IGMF. Since in such a distance from the site of the GRB one typically expects to reach a void, this can serve as a method for estimating the highly uncertain value of the IGMF in voids. A similar suggestion was made by Plaga (1995).

4. DISCUSSION

We have calculated the synchrotron and SSC emission during the prompt GRB from internal shocks and studied the relation between these two components and its dependence on the model parameters. Our analysis takes into account the high-energy cutoffs due to the Klein-Nishina effect, pair production with low-energy photons and the cosmic IR background, and Thomson scattering.

For $p > 2$, the emission above $\sim$100 MeV is typically dominated by the SSC component, while the synchrotron component is dominant at lower energies. If the variability time is $t_v \gtrsim 1$ ms, then $E_p \sim 300$ keV would imply a cutoff at $\sim$30 MeV, and the synchrotron emission would be dominant at all energies. Future observations by *GLAST* may help determine the value of p and whether the high-energy emission is consistent with a single power law or has a break where the νF_ν slope turns from negative to positive. The former would imply that the high-energy emission is dominated by a single component, the synchrotron emission, while the latter implies that the SSC component becomes dominant above a certain energy ($\sim$100 MeV).

The SSC high-energy emission should show a similar variability to that observed in the BATSE range. An additional emission mechanism that might contribute to the high-energy emission is external Compton, which may be relevant if GRBs occur inside pulsar wind bubbles (Guetta & Granot 2003).

In addition, there might be delayed high-energy emission from the internal shocks due to upscattering of CMB photons by $e^\pm$ pairs produced by the interaction between $\gtrsim$300 GeV photons from the prompt GRB and the IR background photons (Dai & Lu 2002). The detection of such emission would be possible only for intergalactic magnetic fields (IGMFs) $\lesssim 10^{-21}$ G at a distance of a few Mpc from the site of the GRB, so that it could serve as a probe for the strength of the IGMF in voids.

As can be seen from equations (11) and (19) and Figure 1, larger values of Γ or t_v shift the cutoff at $h\nu_{\gamma\gamma}$ to larger energies, while at the same time, they imply lower values of E_p. For example, in order to have $\sim$1 GeV photons for $t_v \sim 1$ ms, we need $\Gamma \gtrsim 350$, which in turn implies $E_p \lesssim 100$ keV. If X-ray flashes are GRBs with such parameters, as suggested by Guetta et al. (2001), then we can expect GeV emission from X-ray flashes.

In order to explain the prompt high-energy photons of up to $\sim$3 GeV that were observed in GRB 940217 (Hurley et al. 1994), together with the value of $E_p \approx 200$ keV that was measured for this burst, we need a very small variability time $t_v \sim 0.1$ ms and $\Gamma \sim 600$ (see the solid curve in the bottom panel of Fig. 1). If indeed such high-energy emission is typical for GRBs with E_p in the BATSE range, as can be tested by the future mission *GLAST*, this might suggest very low variability times ($t_v \lesssim 0.1$ ms). This possibility is consistent with the fact that in many GRBs, the shortest measured variability time is limited by the temporal resolution of the instrument, and there is no observational lower limit on t_v. On the other hand, $t_v \sim 0.1$ ms implies a source size $\lesssim ct_v \sim 30t_{v,-4}$ km, so that it is unlikely that t_v can be much smaller than 0.1 ms. Therefore, this might imply a typical variability time of $t_v \sim 0.1$ ms, which may be resolved by Super Agile.

We thank Eli Waxman for useful comments. This research was supported by the partial support of the Italian Ministry for University and Research (MIUR) through the grant Cofin-01-02-43 (D. G.) and by the NSF grant PHY 00-70928 (J. G.). D. G. thanks the Institute for Advanced Study, where most of this research was carried out, for the hospitality and the nice working atmosphere.

REFERENCES

Dai, Z. G., & Lu, T. 2002, ApJ, 580, 1013
Granot, J., Piran, T., & Sari, R. 2000, ApJ, 534, L163
Guetta, D., & Granot, J. 2003, MNRAS, in press
Guetta, D., Spada, M., & Waxman, E. 2001, ApJ, 557, 399
Hurley, K., et al. 1994, Nature, 372, 652
Lithwick, Y., & Sari, R. 2001, ApJ, 555, 540
Panaitescu, A., & Mészáros, P. 2000, ApJ, 544, L17
Papathanassiou, H., & Mészáros, P. 1996, ApJ, 471, L91
Pilla, R. P., & Loeb, A. 1998, ApJ, 494, L167
Plaga, R. 1995, Nature, 374, 430
Rees, M. J., & Mészáros, P. 1994, ApJ, 430, L93
Salamon, M. H., & Stecker, F. W. 1998, ApJ, 493, 547
Sari, R., & Piran, T. 1997, MNRAS, 287, 110
Sari, R., Piran, T., & Narayan, R. 1996, ApJ, 473, 204